Molecular Crystals and Liquid Crystals
Publication details, including instructions for authors and subscription information:
http://www.tandfonline.com/loi/gmcl16

The Contrast Improvement of an Ultrasound Nematic Detector by Means of an Electric Field

A. Strlgazzl [a] & G. Barbero [a]
[a] GNCL, Gruppo Nazionale Cristalli Liquidi, Dipartimento di Fisica, Politecnico, c. Duca degli Abruzzi, 24-10129, Torino, Italia
Version of record first published: 13 Dec 2006.

To cite this article: A. Strlgazzl & G. Barbero (1983): The Contrast Improvement of an Ultrasound Nematic Detector by Means of an Electric Field, Molecular Crystals and Liquid Crystals, 103:1-4, 193-204

To link to this article: http://dx.doi.org/10.1080/00268948308071050

Mol. Cryst. Liq. Cryst., 1983, Vol. 103, pp. 193–204
0026-8941/83/1034–0193/$18.50/0

Printed in the United States of America

The Contrast Improvement of an Ultrasound Nematic Detector by Means of an Electric Field

A. STRIGAZZI† and G. BARBERO‡

GNCL, Gruppo Nazionale Cristalli Liquidi,
Dipartimento di Fisica, Politecnico,
c. Duca degli Abruzzi, 24-10129 Torino, Italia

(*Received February 8, 1983; in final form May 16, 1983*)

In the frame of the continuum theory, the calculation of the hydrodynamic interaction ultrasound–nematic, also in the presence of an electric field, has been carried out. The mean square tilt angle, and consequently, the contrast is shown to be considerably improved, until the electrically controlled birefringence threshold is reached. Experimental measurements of the cell capacitance variations, performed by means of a lock-in amplified bridge method, show the same behavior of the theoretical curve, calculated in some restrictive hypotheses.

I. INTRODUCTION

It is well known that an aligned nematic film can be used in order to obtain both acoustical imaging[1,2] and ultrasound optical detection.[3–5] These properties appear to be an attractive technique to perform some non-destructive testing methods; hence it is interesting to improve the resolution and the sensitivity of the ultrasound–nematic interaction.

Recently the improvement of the response time as well as the sensitivity of an acoustic nematic detector by means of a proper electric field has been shown by Perbet[6] and Kagawa *et al.*[7]

The present paper deals with a homeotropic nematic film used as an ultrasound detector. We show that the contrast can be substantially

†and Facoltà di Medicina Veterinaria, Università, Torino, Italia.
‡and Unical Liquid Crystal Group, Dipartimento di Fisica, Università, Arcavacata di Rende (Cosenza), Italia.

improved by applying a convenient AC-electric field to the cell plates: in particular, the maximum improvement has been obtained near the threshold of the electrically controlled birefringence[8] (ECB).

II. THEORY

The optical contrast[9] of an ultrasound nematic detector, based on the guest-host[10] effect, is expected to be increasing if an electric field of sufficient intensity is applied to the sample. The electric field indeed tends to destroy the undisturbed homeotropic configuration, if the nematic has a negative permittivity anisotropy ($\epsilon_a < 0$), acting as well as the incident ultrasound beam.

These effects are quite different: the ultrasound induces a flow pattern (streaming) also at very low intensity,[5,11] whereas the electric field produces only a static distortion of the nematic director, if it remains below the threshold of the dynamic scattering mode[12] (DSM).

In the presence of only an ultrasound wave vector of low intensity normal to the slab plates, the hydrodynamics of the nematic liquid crystal is described in the steady state by:[13]

$$\begin{aligned} &\eta_1 \partial^2 v_x/\partial z^2 + \mu_1(\partial/\partial z)(\phi_0^{us}\partial v_z/\partial z) = 0 \\ &\partial^2 \phi_0^{us}/\partial z^2 - (\alpha_2/K_{33})(\partial v_x/\partial z) - [(\mu_2 + \mu_3)/K_{33}]\phi_0^{us}\partial v_z/\partial z = 0 \end{aligned} \tag{1}$$

where η_1, α_2 are the Leslie–Ericksen viscosity coefficients ($\alpha_2 < 0$ for commonly used nematics), μ_j are bulk viscosity coefficients, K_{33} is the bend elastic constant, $\mathbf{v}$ and ϕ_0^{us} being respectively the particle velocity and the tilt angle of the director with respect to the z-axis (see Figure 1a). The low intensity ensures that the tilt angle remains small. The continuity equation gives, by restricting ourselves to the incompressibility hypothesis:

$$\operatorname{div} \mathbf{v} = 0 \tag{2}$$

e.g. v_z is independent of z, and then for symmetry is constant in the whole sample.

For the more general case in which the density ρ is not constant, see Appendix 1. In the present hypothesis, system (1) can be written

$$\begin{aligned} &d^2 v_x/dz^2 = 0 \\ &d^2\phi_0^{us}/dz^2 - (\alpha_2/K_{33})\, dv_x/dz = 0 \end{aligned} \tag{3}$$

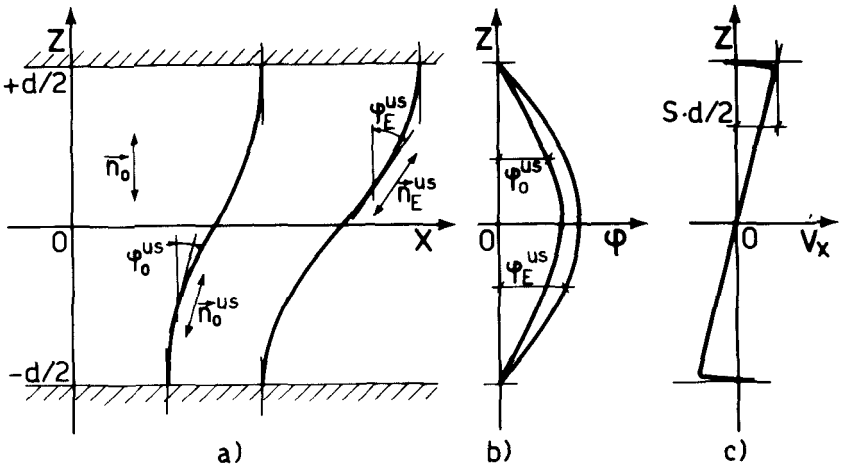

FIGURE 1 (a) director lines in the undisturbed state ($\mathbf{n}_0$), in the presence of ultrasound only ($\mathbf{n}_0^{us}$), and in the presence of both ultrasound and electric field ($\mathbf{n}_E^{us}$); (b) tilt angles vs. z in the previous cases (ϕ_0^{us} ϕ_E^{us}); (c) particle velocity profile in the infinite slab.

ϕ_0^{us} resulting simply dependent on z. Consequently, the tilt angle in the cell due only to the ultrasound field (see Figure 1b; d is the cell thickness) is given by:

$$\phi_0^{us} = -(\alpha_2 S/2K_{33})\left[(d/2)^2 - z^2\right] \tag{4}$$

in the strong anchoring hypothesis, S being the so-called shear rate:[14]

$$v_x = Sz \tag{5}$$

Eq. (5) of course can describe a simplified velocity profile in the whole slab, except in the limit layers at the walls (see Figure 1c), consistent with the picture of the slab as a unique vortex ($v_z = 0$ for any x) while Eq. (4) gives a useful approximation of the tilt angle, for small values of $(\phi_0^{us})_{max} = -\alpha_2 S d^2/8K_{33}$ proportional to the shear rate and consequently to the ultrasound intensity.

The more rigorous analysis performed in Appendix 1 shows that Eq. (4) remains essentially valid. On the other hand, the Euler–Lagrange equation representing the balance between the elastic torque and the electric one, in the presence of only a reorienting electric field normal to the cell plates is obtained as

$$d^2\phi_E^0/dz^2 + \xi_E^{-2}\sin 2\phi_E^0 = 0 \tag{6}$$

ξ_E being the coherence length[15] due to the electric field effect, resulting in

$$\Xi_E^{-2} \equiv \xi_E^{-2} d^2 = V^2/\left(V_{\text{th}}^{\text{ECB}}\right)^2 \equiv u^2 \tag{7}$$

where Ξ_E is the reduced coherence length and u the reduced voltage applied to the cell, V being the applied voltage, and $V_{\text{th}}^{\text{ECB}}$ the threshold one for the ECB effect. Approximate solutions of Eq. (6) are well known, also in the case of generalized coherence lengths.[16]

Let us consider now the presence of both ultrasound wave and electric field: in the previous hypotheses, the torques balancing is given by

$$d^2\phi_E^{\text{us}}/dz^2 + \xi_E^{-2}\sin 2\phi_E^{\text{us}} - (\alpha_2/K_{33})\, dv_x/dz = 0 \tag{8}$$

where the velocity v_x due to both actions is generally different from the one due only to the ultrasound, since the superimposed electric field increases the local tilt angle, the effective viscosity becoming greater.

By neglecting this fact, Eq. (8) becomes

$$d^2\phi_E^{\text{us}}/dz^2 + \xi_E^{-2}\sin 2\phi_E^{\text{us}} + \alpha_2 S/K_{33} = 0. \tag{9}$$

We note that $\phi_E^{\text{us}} = \phi_0^{\text{us}} + \phi_E$, pointing out that $\phi_E \neq \phi_E^0$ in the presence of only the electric field, this latter acting now on a director pattern distorted by ultrasound. By substituting Eq. (3) in Eq. (9), we have finally

$$d^2\phi_E/dz^2 + \xi_E^{-2}\sin\left(\phi_0^{\text{us}} + \phi_E\right) = 0 \tag{10}$$

We point out that Eq. (10) is independent of a particular form of the velocity field imposed by the ultrasound wave: this fact gives generality to our calculation. On the other hand, the interest of Eq. (10) consists in the fact that it shows immediately the orienting action of the electric field, depending only on its coherence length, exerted on the director pattern, distorted hydrodynamically by ultrasound. We point out that the static theory of the ultrasound–nematic interaction would carry out in the presence of an electric field to:

$$d^2\phi_E^{\text{us}}/dz^2 + \left(\xi_E^{-2} + \xi_{\text{us}}^{-2}\right)\sin 2\phi_E^{\text{us}} = 0 \tag{11}$$

ξ_{us} being the ultrasound coherence length,[17,18] by implying the existence of a threshold, which is excluded by Eq. (10), provided ϕ_0^{us} is different from zero.

Let us now find an approximate analytical solution in the case of small values of ϕ_E^{us}.

If $\xi_E \gtrsim d$, e.g. if $V \lesssim V_{th}^{ECB}$, it is possible to stop to the second term the expansion of ϕ_E in the parameter ξ_E^{-1}, getting

$$\phi_E \simeq \phi_E^{(0)} + \xi_E^{-2}\phi_E^{(2)} = \xi_E^{-2}\phi_E^{(2)} \tag{12}$$

Hence, neglecting higher order terms, Eq. (10) gives

$$d^2\phi_E^{(2)}/dz^2 + \sin 2\phi_0^{us} = 0. \tag{13}$$

Since ϕ_0^{us} expressed by Eq. (4), is small, Eq. (13) can be linearized, obtaining finally (see Figure 1b):

$$\phi_E = -\xi_E^{-2}(\alpha_2 S/4K_{33})\left[(z^4/3) - (d^2z^2/2) + (5d^4/48)\right]. \tag{14}$$

It is interesting to point out that the ratio $(\phi_E/\phi_0^{us})_{max} = (5/24)\Xi^{-2} \sim 0.21$ at the threshold of the ECB effect.

Furthermore an observable parameter concerning the director alignment in the nematic cell is the mean square tilt angle $\langle\phi^2\rangle$, which can be detected by capacitance measurements.[19] Moreover, recently Schadt *et al.*[20] have shown that the optical contrast of a guest-host display can be easily determined by means of such a technique, because both capacitance variation and optical contrast are directly related to the mean square tilt angle $\langle\phi^2\rangle$. Hence, it is convenient to compute this observable in our case, resulting:

$$\langle(\phi_0^{us})^2\rangle = (\alpha_2^2 S^2/120K_{33}^2)\, d^4 \tag{15}$$

and, respectively:

$$\langle(\phi_E^{us})^2\rangle = (\alpha_2^2 S^2/120K_{33}^2)\, d^4(1 + 0.926\Xi_E^{-2} + 0.041\Xi_E^{-4}). \tag{16}$$

Finally, the ratio between the mean square tilt angle in the presence of both ultrasound and electric field, and the one in the presence of the acoustic wave only is obtained as

$$\langle(\phi_E^{us})^2\rangle/\langle(\phi_0^{us})^2\rangle = 1 + 0.926\Xi_E^{-2} + 0.041\Xi_E^{-4} \tag{17}$$

and results independent of the acoustic intensity, depending only on the reduced voltage u applied to the nematic cell (within an error of $\sim 5\%$, such a ratio vs. the reduced voltage has a parabolic behavior).

Conversely, $\langle(\phi_0^{us})^2\rangle$ is shown to be increasing with the square shear rate S^2, e.g. with the acoustic intensity.

Moreover, the relative capacitance variations $\delta C/C_{\parallel}$, where $C_{\parallel}$ is the capacitance of the homeotropic cell, follow the same behavior, since they are proportional to the mean square tilt angles $\langle\phi^2\rangle$.

On the other hand, the function $\delta C/C_{\parallel}$ vs. (η, V) expresses a sensitive dependence of $\langle\phi^2\rangle$ on both parameters: this means that, by doping the negative nematic with a dye, for example of the *p*-type (e.g. a dye with its transition moment almost parallel to its molecular axis) realizing in this way a guest-host system, it is possible to improve substantially the optical contrast of the display, acting as an ultrasound detector, by applying a convenient simultaneous electric field.

In particular the mean optical density being defined by[10,20]

$$\langle\alpha\rangle \simeq \alpha_{\parallel} - \alpha_a\langle\phi^2\rangle \tag{18}$$

where $\alpha_{\parallel}$ is the optical density of an ideal homeotropic sample, and α_a is the optical density anisotropy, the optical contrast is obtained as:[23]

$$c \equiv 1 - \langle\alpha\rangle/\alpha_{\parallel} = (1 - 1/r)\langle\phi^2\rangle \tag{19}$$

where $r \equiv \alpha_{\parallel}/\alpha_{\perp}$ is the dichroic ratio of the dye. Consequently, the gain defined as:

$$g \equiv (c_E^{us}/c_0^{us}) - 1 \tag{20}$$

giving the improvement between the contrast value at the ECB-threshold and the one in the absence of an electric field, results to be given by

$$g = (\delta C/\delta C_0^{us}) - 1 \tag{21}$$

independent of the dichroic ratio. By taking into account Eqs. (15) and (16) we conclude finally that

$$g \simeq 0.926\Xi_E^{-2}(1 + 0.044\Xi_E^{-2}) \tag{22}$$

e.g. with a maximum error of 5%:

$$g \simeq \Xi_E^{-2} \tag{23}$$

Hence the gain is predicted to be dependent essentially on the ECB effect.

III. EXPERIMENT

Systematic measurements of the capacitance have been performed on a homeotropic nematic cell with thickness 50 μm, realized with two glass plates covered by a thin deposit of tin oxide, sealed by araldite and filled through a hole by anhydrous MBBA in controlled atmosphere.

The experimental set up, described in another paper,[21] uses an AC-bridge method. The bridge is driven by an audio-frequency sinusoidal voltage, low enough to produce no detectable distortion in the sample (1500 Hz, 0.3 V_{pp}). The bridge output is amplified by a lock-in, obtaining a resolution of $\sim 10^{-5}$ on the capacitance.

A low-frequency bias voltage V ($\sim$ 67 Hz), having no harmonic components neither with the bridge driving voltage nor with the line can be applied to the sample with preselected values. Actually, the values of the bias voltage have been chosen in order to cover the whole range between zero and the dynamic scattering mode threshold V_{th}^{DSM}.

The ultrasound beam is applied normally to the nematic cell by a PZT5A-transducer (2.4 MHz), coupled with the cell by means of a thin silicon oil layer.[22] The transducer is excited by a sinusoidal RF-voltage (2.4 MHz, 78 V) modulated by a 200 Hz—square wave, in

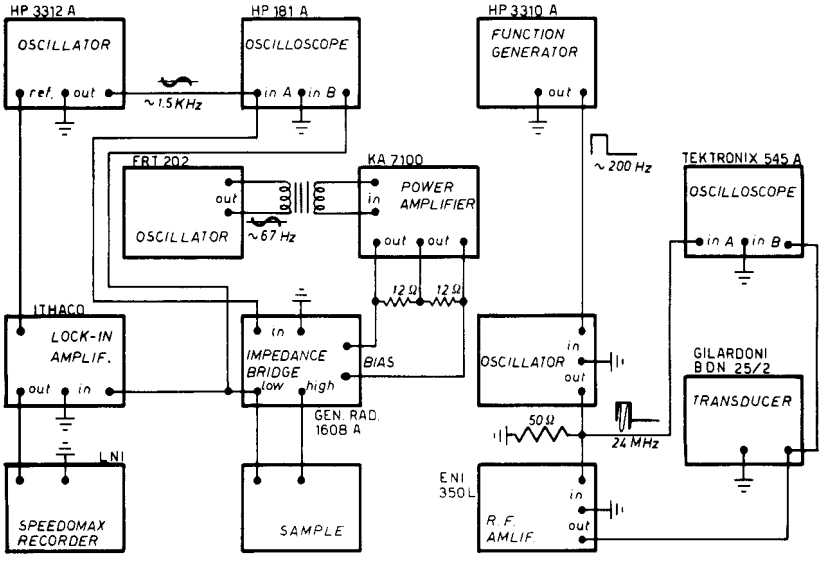

FIGURE 2 Experimental set-up.

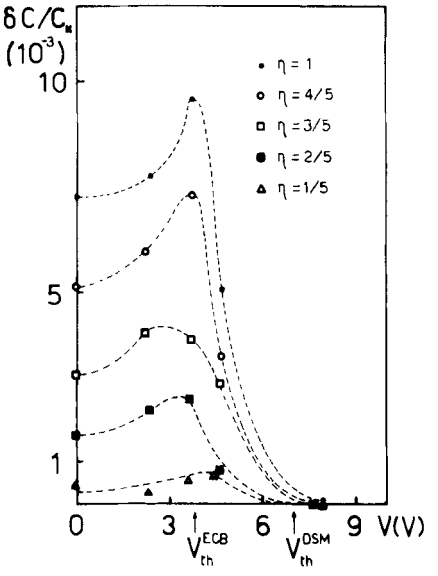

FIGURE 3 Relative capacitance variations $\delta C/C_{\perp}$ vs. the voltage V applied to the cell and the acoustic intensity: experimental data. Dotted lines are indicative only.

order to get a prefixed duty cycle η, ranging between $0 \leftrightarrow 1$. Note that if $\eta = 1$ the acoustic intensity incident on the nematic has been evaluated as $I \simeq 1.0$ W/cm^2.

The irradiation time is ~ 10 s, to avoid the heating of the sample. The measurements have been performed at room temperature ($\sim 24°$C).

The experimental apparatus is shown in Figure 2; moreover, the experimental data are reported in Figure 3.

IV. DISCUSSION

By considering Figure 3, we point out that:

(a) the relative capacitance variation $\delta C/C_{\perp}$ is an increasing function of the duty cycle, as may be expected,[11] the duty cycle being proportional to the acoustic intensity I;

(b) $\delta C/C_{\perp}$ increases substantially as V increases between 0 and V_{th}^{ECB};

(c) $\delta C/C_{\perp}$ reaches its maximum value for $V \simeq V_{th}^{ECB}$;

(d) $\delta C/C_{\parallel}$ drops rapidly to zero as well as V increases between V_{th}^{ECB} and the threshold of the dynamic scattering mode V_{th}^{DSM}.

This behavior results in reasonable agreement with the prediction of the analytical calculation carried out in Section II, concerning the range between 0 and V_{th}^{ECB}. The values of $\delta C/\delta C_0^{us}$ predicted by Eq. (17) are reported in Figure 4, and compared with the experimental points written with their standard deviations. We note, the theory predicts the increasing parabolic behavior of $\delta C/\delta C_0^{us}$ vs. u expressed by the experimental data, but overestimates the crossed effect ultrasound–electric field in the nematic slab, due to the restrictive hypotheses, we have introduced for solving the problem analytically.

On the contrary, the previous theory does not apply to the condition existing between V_{th}^{ECB} and V_{th}^{DSM}, since such a calculation neglects the presence of the electric conductivity. Nevertheless, it is easy to understand that the presence of an ultrasound beam in a nematic film subjected to the DSM, does not change the director configuration

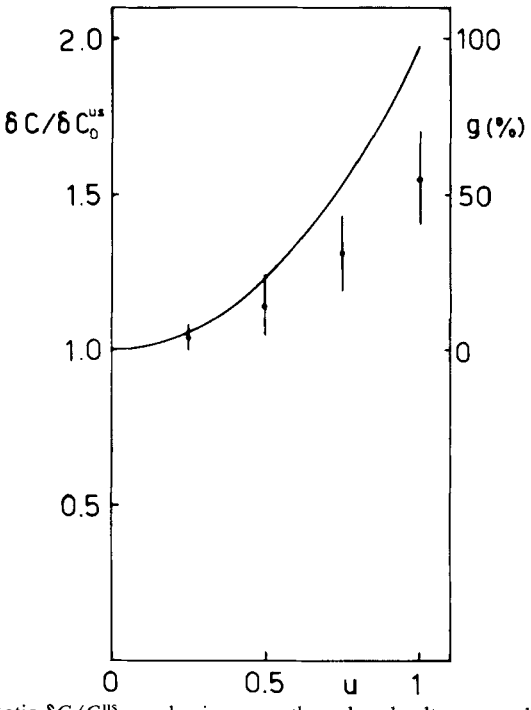

FIGURE 4 Ratio $\delta C/C_0^{us}$—and gain g—vs. the reduced voltage u applied to the cell: experimental data and theoretical predictions (full line).

due to the latter effect, because the DSM reaches rapidly a situation characterized by the maximum allowed disorder, i.e. the permittivity goes to $\langle\epsilon\rangle = (1/3)(\epsilon_{\parallel} + 2\epsilon_{\perp})$ as well as V increases above $V_{\text{th}}^{\text{DSM}}$.

We point out that by Eq. (21) Figure 4 shows also the predicted behavior of the gain vs. the reduced voltage compared with the experimental one.

In conclusion, the nematic–ultrasound interaction in the presence of an electric field has been investigated. In some restrictive hypothesis—the most severe of which is the assumption of the cell as an infinite slab subjected to planar ultrasound wave—approximated analytical solutions of the constitutive equations have been given.

The experimental data are in reasonable agreement with the predictions of our calculation, for small values of the duty cycle ($\eta \lesssim 0.5$): on the contrary, for relatively higher ultrasound intensities ($I \gtrsim 500$ mW/cm^2) our hypothesis of small tilt angle becomes a imprecise approximation.

APPENDIX 1

By dropping out the incompressibility hypothesis, the continuity equation in the steady state becomes

$$\operatorname{div}(\rho \mathbf{v}) = 0 \tag{2'}$$

If the sample is a slab subjected to a planar ultrasound wave normal to the boundary walls, $\rho\mathbf{v}$ is independent of x, and consequently

$$\rho \propto v_z^{-1} \tag{2''}$$

Hence system (1) assumes the form

$$\eta_1 \, dv_x/dz + \mu_1 \phi_0^{\text{us}} \, dv_z/dz = \tau$$

$$d^2\phi_0^{\text{us}}/dz^2 + \left(\frac{\mu_2 + \mu_3}{\mu_1 K_{33}} \eta_1 - \frac{\alpha_2}{K_{33}} \right) dv_x/dz = \tau \frac{\mu_2 + \mu_3}{\mu_1 K_{33}} \tag{3'}$$

being $\tau = \eta_1 (dv_x/dz)_{z = \pm d/2}$ the tangential stress at the wall imposed by the ultrasound[24] in the strong anchoring hypothesis. In order to take into account the boundary condition $v_x(\pm d/2) = 0$, the function $v_x(z)$ can be expanded in power series of $z \equiv 2z/d$. Symmetry considerations give $v_x(z)$ as an odd function of z; by restricting ourselves

only to the first terms, we obtain

$$v_x(z) = S_0(d/2)[1 - z^2]^2 z \tag{5'}$$

Eq. (5') gives $v_x(\pm 1/2) = 0$ are required, and

$$(dv_x/dz)_{z=\pm 1/2} = 0$$

consistent with the condition $\tau = 0$ at the interfaces solid-NLC. In (5') $S_0 = (dv_x/dz)_{z=0}$ is the shear-rate in the mid-point of the cell, depending on the boundary stress. By substituting Eq. (5') into system (3') we deduce, being $\mu_1 \simeq \mu_2 \simeq \mu_3$:

$$\varphi_0^{us}(z) = -S_0 d^2[(2\eta_1 - \alpha_2)/8K_{33}]\{z^2(1 - z^2) - (1 - z^6)/3\} \tag{4'}$$

If $z^6 \ll 1 \Rightarrow z < 1/2$, eq. (4') gives

$$\varphi_0^{us} = S_0 d^2[(2\eta_1 - \alpha_2)/8K_{33}](1 - z^2) - S_0 d^2(2\eta_1 - \alpha_2)/24K_{33} + 0(z^4) \tag{4''}$$

Since the first term of Eq. (4'') is the analogous one of (4), we observe that Eq. (4) is valid only in the central region of the cell ($z \lesssim 0.6 \Rightarrow 0(z^4) \lesssim 10\%$). On the other hand by using (4'), after trivial calculation, it is easy to show that

$$\langle(\varphi_0^{us})^2\rangle \simeq S_0^2 d^4(2\eta_1 - \alpha_2)^2/1690K_{33}^2 \tag{15'}$$

In order to compare relations (15') and (15) we observe that for MBBA it results[13] $\eta_1 = 1.035$ poise and $-\alpha_2 = 0.78$ poise. Consequently Eq. (15') can be rewritten as

$$\langle(\varphi_0^{us})^2\rangle \simeq S_0^2 d^4 \alpha_2^2/127K_{33}^2 \tag{15''}$$

in good agreement with the above mentioned eq. (15)

Acknowledgment

This work has been partially supported by the Centro Ricerche FIAT S.p.A.

References

1. S. Nagai and K. Iizuka, *Japan. J. Appl. Phys.*, **17**, 723 (1978).
2. S. Nagai and K. Iizuka, *Mol. Cryst. Liq. Cryst.*, **45**, 83 (1978).
3. S. Nagai, A. Peters and S. Candau, *Rev. Phys. Appliquée*, **12**, 21 (1977).
4. C. Sripaipan, C. F. Hayes and G. T. Fang, *Phys. Rev. A*, **15**, 1297 (1977).
5. J. N. Perbet, M. Hareng, S. Le Berre and B. Mourey, in: GNCL "Cristalli liquidi" Proc. UNICAL 1981 (CLUT, Torino, 1982) p. 747.
6. J. N. Perbet, M. Hareng and S. Le Berre, *Rev. Phys. Appliquée*, **14**, 569 (1979).
7. Y. Kagawa, T. Hatekeyama and Y. Tanaka, *J. Sound. Vibr.*, **36**, 407 (1974).
8. E. B. Priestley, P. J. Wojtowicz and Ping Sheng, *Introduction to Liquid Crystals* (Plenum Press, New York, 1975), p. 115.
9. G. Barbero and A. Strigazzi, *Applied Physics*, **A31**, 55 (1983).
10. S. Aftergut and H. S. Cole, Jr., *Appl. Phys. Lett.*, **38**, 599 (1981).
11. A. Strigazzi and G. Barbero, this conference D-5P, p. 175.
12. P. A. Penz and G. W. Ford, *Phys. Rev. A*, **6**, 414 (1972).
13. S. Nagai and K. Iizuka, *Japan. J. Appl. Phys.*, **13**, 189 (1974).
14. T. Carlsson, *Mol. Cryst. Liq. Cryst.*, **89**, 57 (1982).
15. H. Kelker and R. Hatz, *Handbook of Liquid Crystals* (Verlag Chemie, Weinheim, 1980).
16. G. Barbero, R. Malvano and A. Strigazzi, *Il Nuovo Cimento*, **59B**, 367 (1980).
17. J. L. Dion and A. D. Jacob, *Appl. Phys. Lett.*, **31**, 490 (1977).
18. G. Barbero and A. Strigazzi, *Mol. Cryst. Liq. Cryst. Lett.*, **82**, 5 (1982).
19. G. Barbero and A. Strigazzi, *Mol. Cryst. Liq. Cryst. Lett.*, **72**, 211 (1982).
20. M. Schadt and P. Gerber, *Mol. Cryst. Liq. Cryst.*, **65**, 241 (1981).
21. G. Barbero and A. Strigazzi, *Il. Nuovo Cimento*, **64B**, 101 (1981).
22. A. Strigazzi, *Lett. Nuovo Cimento*, **24**, 255 (1979).
23. F. Ghara Djedaghi and R. Voumard, *J. Appl. Phys.*, **53**, 7306 (1982).
24. C. Hayes, *Mol. Cryst. Liq. Cryst.*, **59**, 317 (1980).